# Synergism of Au and Ru Nanoparticles in Low-Temperature Photoassisted CO 2 Methanation

Diego Mateo, Déborah de Masi, Josep Albero, Lise-Marie Lacroix, Pier-Francesco Fazzini, Bruno Chaudret, Hermenegildo Garcia

# Synergism of Au and Ru nanoparticles in low temperature photo-assisted $CO_2$ methanation.

Diego Mateo,[a] Deborah De Masi,[b] Josep Albero,[a] Lise-Marie Lacroix,[b] Pier-Francesco Fazzini,[b] Bruno Chaudret,*[b] and Hermenegildo García*[a]

**Abstract:** Au and Ru nanoparticles have been deposited on Siralox® substrate by impregnation and chemical reduction, respectively (Au-Ru-S). The as-prepared material has demonstrated to be very active for the selective $CO_2$ metanation to $CH_4$ at temperatures below 250 °C. In addition, Au-Ru-S exhibits $CH_4$ production enhancement upon UV-Vis light irradiation starting at temepratures higher than 200 °C, although the contribution of the photoassisted pathway of $CH_4$ production decreases as temperature increases. Thus, a maximum $CH_4$ production of 204 mmol/$g_{Ru}$ at 250 °C upon 100 mW/cm$^2$ irradiation was achieved. Control experiments using Ru-S and Au-S materials revealed that Ru nanoparticles are the $CO_2$ methanation active sites, while Au NPs contribute harvesting light, mainly visible as consequence of the strong Au plasmon band centrered at 529 nm. The visible light absorbed by Au NPs plasmon could act as local heaters of neighbouring Ru NPs, increasing their temperature and enhancing $CH_4$ production.

## Introduction

The development of new approaches for the production of environmentally friendly and cheap fuels using renewable energy sources has become a topic of paramount importance in order to diminish $CO_2$ emissions, minimizing the impact of global warming derived from the massive use of fossil fuels.[1] In this regard, different technologies have emerged in order to capture and store solar energy such as photovoltaics, photothermal, etc.[2] Among them, photocatalysis has been proposed as a possible approiach to convert directly Sunlight into chemical energy.[3] The aim of photocatalysis is to harvest the abundant, clean, and safe energy from sunlight, storing it into chemical bonds of compounds that could be used as fuels. These *solar fuels* would deliver their energy on demand in a stable and reproducible way independently of the weather conditions and daytime.

Efficient photocatalytic solar fuels production depends on the development of affordable and stable photocatalysts, these being a growing interest in this area.[4] The most widely used photocatalysts have been based on semiconductor materials having convenient energy bands that have been typically modified by deposition of suitable noble metal based co-catalysts in order to improve charge separation and/or increase the production rates and efficiencies of the photocatalysts. Co-catalysts for hydrogen evolution are generally Pt and other noble metals, while oxygen evolution has been frequently enhanced by metal oxides such as $IrO_2$, CoO, $RuO_2$ being one of the preferred options.[5]

Hydrogenation is one of the few exothermic reactions having $CO_2$ as substrate and can render a series of C1 products and light hydrocarbons that have large interest as fuels and as feedstocks of the chemical industry.[6]

Power to gas or power to liquid fuels production have been found a suitable approach for hydrocarbons synthesis through Fischer-Tropsch or Sabatier reactions.[7] The Sabatier reaction, as it is known the $CO_2$ methanation, is a well-stablished industrial process for converting $CO_2$ to $CH_4$ according to Equation 1. $CO_2$ methanation is thermodynamically downhill, although it requires temperatures higher than 250 °C (typically between 300 - 500 °C) to achieve measurable reaction rates due to the high activation energy of the process.[8]

$$CO_2 + 4H_2 \leftrightarrow CH_4 + 2H_2O \qquad \Delta_rH_{298} = -165 \text{ kJ/mol} \quad \text{(Eq. 1)}$$

The list of catalysts that can be employed to promote this reaction are composed by metal oxides such as $Al_2O_3$, $SiO_2$, $ZrO_2$ or $CeO_2$ as supports and metal nanoparticles (NPs) based on Ru, Fe, Ni, Co, Rh, among others as catalytic sites.[8] One of the most active and preferred metal is Ru due to its high selectivity towards $CH_4$, high activity even at relatively low temperatures, and high stability to the ambient and reaction conditions.[9]

In contrast to thermal catalysis where supported Ru NPs is widely used, photocatalytic $CO_2$ methanation has made ample use of molecular Ru complexes. These Ru complexes exhibit a strong visible absorption band and can act as photosensitizers of

[a] Mr. D. Mateo, Dr. J. Albero and Prof. H. Garcia
Instituto Universitario de Tecnología Química CSIC-UPV, Universitat Politècnica de València, Av. de los Naranjos s/n, 46022, Valencia, Spain.
E-mail: hgarcia@qim.upv.es

[b] Ms. D. Masi, Dr. L.-M. Lacroix, Prof. P.-F. Fazzini and Prof. B. Chaudret
Laboratorie de Physique et Chemie des Nano-Objets
UMR5215 INSA-CNRS
Institut des Science Appliquèes
135 avenue de Rangueil 31077 Toulouse (France)
E-mail: chaudret@insa-toulouse.fr

Supporting information for this article is given via a link at the end of the document.

metal oxides or other wide bandgap semiconductor materials, such as MOFs, in order to introduce visible light photoresponse in the photocatalytic system.[10] Only a small number of articles have reported that metallic Ru NPs have also photothermal activity for $CO_2$ methanation due to their capability to activate $H_2$ on the surface of these Ru NPS. In one of these reports, it has been shown that upon visible light excitation, Ru NPs supported on a double layered hydroxide (DLH) can reach very high local temperatures, resulting in very efficient $H_2$ activation and, therefore, initiating $CO_2$ methanation.[11] In a different approach, magnetic Fe (0) NPs were coated with a thin discontinuous Ru (0) overlayer forming Fe@Ru core-shell NPs that have demonstrated to be able to promote efficiently the Fischer-Tropsch synthesis upon the excitation of an external magnetic field that causes the heating of the Fe@Ru NPs.[12]
In this manuscript, another example of photothermal $CO_2$ methanation will be described by using a material containing independent Au and Ru metal NPs supported in the commercial inert aluminosilicate, namely Siralox®, (Au-Ru-S).
In the Au-Ru-S system, photoassisted $CO_2$ methanation occurs under UV-Vis light irradiation at temperatures below 250 $^{o}$C. Au NPs are well-known to exhibit plasmonic band in the visible region of the spectrum around 530 nm. Evidence supports that in Au-Ru-S system, the Ru NPs act as active and selective $CO_2$ methanation sites, while due to their plasmonic band Au NPs act as light harvesters of visible light. The energy absorbed by the Au plasmon band is transferred to the Ru NPs in close contact increasing locally their temperature and, therefore, the rate of the $CO_2$ methanation process reaching a $CH_4$ production rate of up to 47.2 mmol/g·h at 200 $^{o}$C under 1000 W/m$^2$ irradiation.

## Results and Discussion

### Photocatalyst characterization

Preparation of the Au-Ru-S photocatalyst is described in the experimental section. In brief, colloidal Au NPs were formed by reduction of $HAuCl_4$ in the presence of oleylamine (OA). TEM image of stabilized Au(OA) NPs are shown in Figure S1a in supporting information. Measurement of a statistically relevant number of Au(OA) shows that their average particle size of 13.5 ± 0.9 nm. These Au(OA) NPs exhibit a plasmon band centered at 529 nm as can be seen in Figure S1b in supporting information. Then, the Au(OA) NPs were deposited by impregnation method on Siralox®, obtaining the Au-S material. Figure 1a shows a HRTEM image of Au-S sample. In this, the presence of round NPs can be observed. The inset in Figure 1a corresponds to a magnification of one of these NPs, where a high degree of crystallinity can be confirmed by the presence of the characteristic diffraction lines. Measurement of the distance between planes resulted in 0.232 nm, corresponding to the 111 facet of metal Au, as reported before.[13] Finally, Ru(COD)(COT) (COD: 1,5-cyclooctadiene; COT: 1,3,3-cyclooctatriene) was reduced on the Au-S surface by $H_2$ in THF at room temperature, obtaining the Au-Ru-S photocatalyst (Figure 1b). In the HRTEM image, the presence of NPs with two different sizes can be observed. The bigger NPs correspond to the Au NPs, while smaller NPs should correspond to Ru NPs. The average particle size of the Ru NPs was 1.2 nm, these were measured by using a methodology previously reported.[14] It is worth noting that the Ru NPs are considerably much smaller than Au(OA) NPs as observed in HRTEM image in Figure 1b. In order to confirm the presence of both Au and Ru NPs supported in Siralox®, elemental mapping of Au-Ru-S sample was carried out, and the results are presented in Figure 2. As can be observed, the presence of Si from the Siralox support can be observed along the sample, while Ru and Au can be distinguished as domains on the substrate.

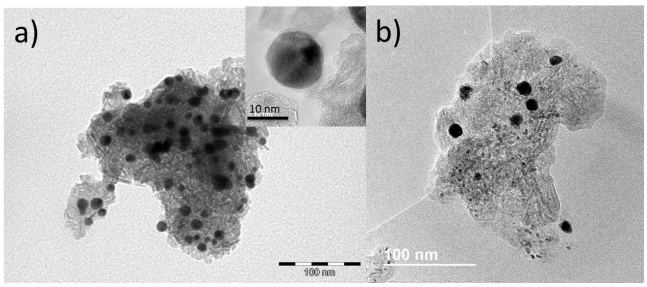


**Figure 1.** HRTEM images of the Au-S (a) and Au-Ru-S photocatalysts (b). Inset corresponds to magnified Au NPs supported on Siralox ®.

The Au and Ru loading in the Au-Ru-S photocatalyst was determined by ICP-OES, obtaining Au and Ru contents of 4.3 and 0.3 wt %, respectively. To visualize the close contact of Au and Ru NPs in Au-Ru-S, dark-field STEM images were recorded. To illustrate the results, Figure S2 in the supporting information shows a representative image of an Au NP in which the presence of smaller Ru NPs, some of them clearly on the Au surface, can be clearly observed. It should be commented that this close contact between the Au NP harvesting light and converting it into heat and Ru NPs being heated and acting as methanation centers is crucial to develop an efficient photothermal catalyst.
The XRD pattern of the Au-Ru-S photocatalyst is presented in Figure 3 and it confirms the presence of metallic Au and Ru NPs based on the position of the diffraction peaks. In Figure 3, the diffraction peaks at 2Θ values of 38, 44, 64, 77 and 82 $^{0}$ correspond to Au (0), while, some diffraction peaks due to $Al_2O_3$ in the Siralox ® support at 46 and 66 $^{0}$ were also identified. More difficult was identification diffraction peaks attributable to Ru (0) due to its low content in the Au-Ru-S sample. The main diffraction peak corresponding to Ru (0) should have appeared at 44 $^{0}$, overlapping with the 44 $^{0}$ Au peak. However, a broad diffraction corresponding to Ru (0) at 84 $^{0}$ can be clearly observed in the high angle region.

**Photothermal methanation**

The Au-Ru-S photocatalyst was placed in a quartz photoreactor that was loaded with $CO_2$ and $H_2$ in a 1:4 stoichiometric ratio according to the requirements of Equation 1 at a total pressure of 1.3 bar. The photoreactor was then heated at different temperatures in the range from 150 to 250 $^{o}$C, and submitted to irradiation with a 300 W Xe lamp. Since the spectral response of the Xe lamp includes from UV to NIR, unavoidable heating of the photocatalyst inside the reactor occurs, as consequence of the illumination. For this reason and to determine the real temperature at the photocatalysts upon light irradiation and external heating, the temperature was measured with an infrared thermometer. The measured values are included in Table 1. In this regard, the reaction temperatures indicated in the manuscript correspond to real ones measured by the infrared thermometer. The irradiation only started after temperature stabilization. The $CH_4$ evolution and the reaction conditions have been summarized in Table 1.

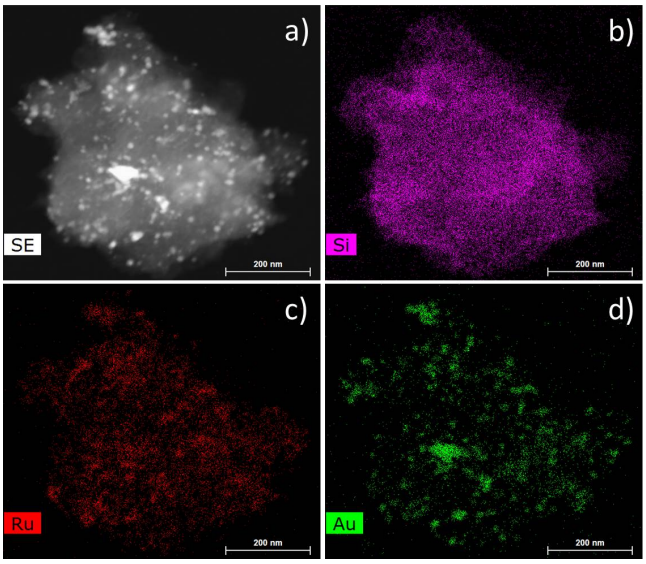


**Figure 2.** STEM image of Au-Ru-S photocatalyst acquired in dark field and elemental mapping of the same region showing exclusively the presence of Si (b), Ru (c) or Au (d), respectively.

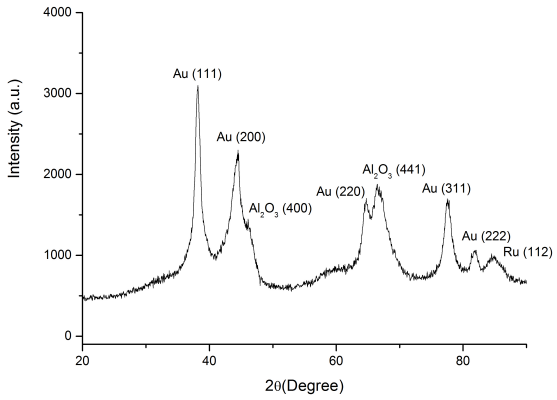


**Figure 3.** XRD of the Au-Ru-S sample.

The $CH_4$ evolution using Au-Ru-S material was measured at different reaction temperatures under dark conditions as can be observed in Table 1 (entries 10, 11 and 12). The $CH_4$ production increased with temperature as expected. It is worthy noticing that these experiments were carried out with the Xe lamp on, but covering the phororeactor with an aluminum foil. In this way, heat contribution from Xe lamp was still present, although the Au-Ru-S catalysts was under dark conditions. Also preliminary experiments irradiating the $CO_2/H_2$ mixture at 200 $^{o}$C in the absence of catalyst showed no $CH_4$ formation, indicating that the stainless steel photoreactor body has no catalytic activity.

The presence of other reaction products such as CO, $CH_3CH_3$, or other light hydrocarbons was not detected under these conditions, and thus, we can assert that the Au-Ru-S material is selective for $CH_4$, following Equation 1, at reaction temperatures between 217.6 and 276.6 $^0$C under dark conditions.

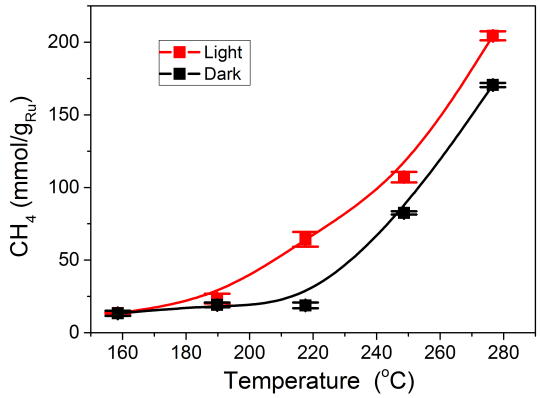


**Figure 4** $CH_4$ evolution at different temperatures using Au-Ru-S photocatalyst under 100 mW/cm$^2$ irradiation (red) and dark (black). $P_{CO2}$=0.25, $P_{H2}$=1.05. Photocatalyst 20 mg (Ru 0.4 wt%, Au 4.4 wt%). Reaction time: 2 h. Red and black lines indicate production trend.

**Table 1.** Ru content, applied and real temperature, reaction time and $CH_4$ formation upon 100 mW/cm$^2$ irradiation using a 300 W Xe lamp for the photoassisted $CO_2$ methanation reaction. The total photocatalyst loading was 20 mg. $P_{H2}$ = 1.05 bar, $P_{CO2}$ = 0.25 bar

| Entry | Sample | Time (h) | Ru content (mg) | Applied and real temperature ($^o$C)[d] | $CH_4$ (mmol/$g_{Ru}$) |
|---|---|---|---|---|---|
| 1 | Au-Ru-S | 2 | 0.042 | 150 (158.5) | 13.52 |
| 2 | Au-Ru-S | 2 | 0.041 | 175 (189.8) | 23.55 |
| 3 | Au-Ru-S | 2 | 0.042 | 200 (217.6) | 64.33 |
| 4 | Au-Ru-S | 2 | 0.042 | 225 (248.6) | 107.17 |
| 5 | Au-Ru-S | 2 | 0.042 | 250 (276.6) | 204.38 |
| 6 | Au-Ru-S | 1 | 0.042 | 200 (217.6) | 36.93 |
| 7 | Ru-S | 1 | 0.098 | 200 (217.6) | 30.17 |
| 8 | Au-S | 1 | 0.92 [d] | 200 (217.6) | 0.373 [d] |
| 9 | Ru-S[a] | 1 | 0.098 | 200 (217.6) | 20.44 |
| 10 | Au-Ru-S[a] | 2 | 0.042 | 200 (217.6) | 18.8 |
| 11 | Au-Ru-S[a] | 2 | 0.038 | 225 (248.6) | 82.49 |
| 12 | Au-Ru-S[a] | 2 | 0.039 | 250 (276.6) | 170.55 |
| 13 | Au-Ru-S | 2 | 0.042 | 25 (58.7) | -[b] |
| 14 | Au-Ru-S[c] | 2 | 0.042 | 25 (58.7) | -[b] |
| 15 | Au-Ru-S[c] | 2 | 0.046 | 200 (217.6) | 12.45 |

[a] dark conditions. [b] undetectable $CH_4$ formation. [c] photocatalyst preactivated at 200 $^0$C for 2 h under $H_2$ atmosphere before reaction.[d] Referred to Au content (mg). [d] values in brackets correspond to the temperature measured at the photocatalyst that is achieved by the combination of external heating and light irradiation.

However, the $CH_4$ production was found increasing when Au-Ru-S photocatalyst was illuminated with a 300 W Xe lamp at 100 mW/cm$^2$, as can be observed in Figure 4 and Table 1 (entries 1 – 5).

The $CH_4$ evolution under light irradiation also increased with the temperature as can be seen in Table 1 comparing entries 1 to 5 and Figure 4, however, it is worthy noticing that the $CH_4$ production at 158.5 $^0$C was very low under light and dark conditions, and therefore, light influence in the methanation reaction using the Au-Ru-S photocatalyst is only notable at temperatures higher than 217.6 $^0$C. On the other hand, as it can be seen in Table 1 and Figure 4, $CH_4$ production at 217.6 $^o$C increases further a 71 % upon light irradiation. However, the contribution of light irradiation to the $CH_4$ production decreases as temperature increases, and thus, the enhancement is of 23 and 17 % as the reaction temperature is 248.6 or 276.6 $^o$C, respectively.

While undetectable amounts of $CH_4$ were found at room temperature under irradiation (Table 1 entry 13), a maximum $CH_4$ production of 204.38 mmol/$g_{Ru}$ was found at 276.6 $^o$C (Table 1, entry 5). The TON after 2 h reaction at 276.6 $^o$C under 100 mW/cm$^2$ calculated by dividing the moles of formed $CH_4$ by the moles of Ru present in the catalyst was of 57.6.

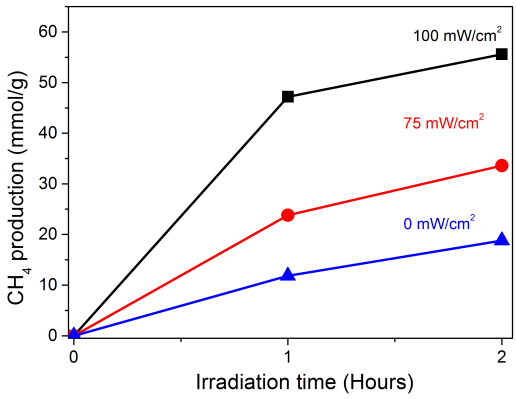


Figure 5. $CH_4$ production using Au-Ru-S photocatalyst at 217.6 $^0$C upon different light intensities. $P_{CO2}$=0.25, $P_{H2}$=1.05. total photocatalyst amount 20 mg (Ru 0.2 wt%, Au 4.1 wt%).

From the influence of the reaction temperature at the initial reaction rate an apparent activation energy of 25.83 kJ/mol was estimated for photothermal $CO_2$ methanation under Xe lamp illumination using Au-Ru-S as photocatalyst.

The influence of the light intensity was also studied, since this experiment provides firm and convincing evidence of photoassistance, even if there is some thermal, dark contribution. In this study $CO_2$ methanation was carried out using Au-Ru-S at 217.6 $^o$C illuminating with different light intensities (Figure 5).

From Figure 5, it can be confirmed that light promotes $CO_2$ methanation, as it can be deduced from the clear dependence of methane production with light intensity. Thus, the $CH_4$ production was very small at 217.6 $^o$C in the dark. However under light intensity of 75 mW/cm$^2$ $CH_4$ production reached 30 mmol×g$^{-1}$. From this threshold, the $CH_4$ evolution increased rapidly up to light intensity values of 100 mW/cm$^2$.

In order to confirm the origin of the $CH_4$ production in the photoassisted pathway, isotopic $^{13}CO_2$ labelling experiments were carried out at 217.6 $^o$C upon 100 mW/cm$^2$, the analyzing products after 2 h reaction by GC-MS spectroscopy were compared with the products obtained from reaction with unlabeled $CO_2$ under identical conditions (Figure S3 in supplementary information). The analysis shows the formation of $^{13}CH_4$ with *m/z* =17. Quantitative analysis of the peak at m/z=16 after subtracting the contribution of $OH^+$ from $H_2O$ indicates that over 90 % should correspond to $^{13}CH_3^+$ ion and, therefore, the formation of $^{12}CH_4$ should be about 10 %, probably due to C scrambling with some organic contaminants present in the photoreactor.

An interesting information was inferred from the time-$CH_4$ formation plot. The temporal evolution of $CH_4$ using Au-Ru-S at 217.6 $^o$C under 100 mW/cm$^2$ irradiation and dark conditions is shown in Figure 6.

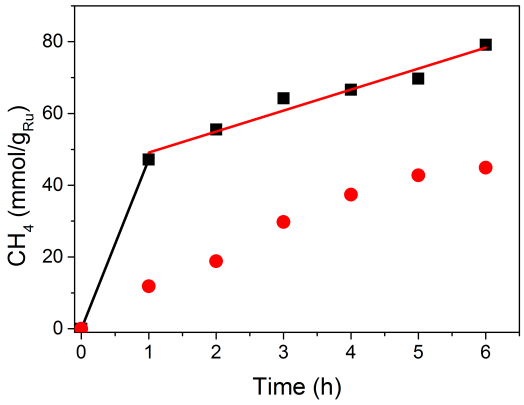


**Figure 6.** $CH_4$ evolution using Au-Ru-S photocatalyst in methanation reaction at 217.6 °C under 100 mW/cm$^2$ (black squares) and dark conditions (red dots). $P_{CO2}$=0.25, $P_{H2}$=1.05. Photocatalyst 20 mg (Ru 0.4 wt%, Au 4.4 wt%).

As can be observed from Figure 6, two different regimes can be clearly differentiated from the $CH_4$ production temporal profile upon light irradiation. During the first reaction hour a production rate of 47.2 mmol/$g_{Ru}$·h was measured, however in the following hours the rate decreased to 5.8 mmol/$g_{Ru}$·h, remaining constant for at least 5 h reaction. The occurrence of deactivation after the initial reaction time with observation of two different regimes has been previously reported in other photoassisted methanation reactions and attributed to the deactivation effect caused by the formation of $H_2O$ as the reaction starts.[15] In order to confirm the stability of metal NPs, dark-field STEM images of the Au-Ru-S photocatalyst before and after reaction were compared. Figure S4 in supplementary information presents representative images of these two samples. As can be observed, no meaningful differences could be observed, neither for the Au nor for the Ru NPs.

**Reaction mechanism**

In order to elucidate the origin of the catalytic activity of Au-Ru-S and particularly if Ru-H could be the intermediate whose formation would require high temperatures, pre-activation of the photocatalyst before reaction was carried out at 217.6 °C under $H_2$ atmosphere for 2 h. Then, the Au-Ru-S was allowed to cool at room temperature before loading $CO_2$:$H_2$ at 1:4 stoichiometric ratio. Then, after presumed Ru-H formation, the photoassisted methanation was attempted at room temperature using pre-activated Au-Ru-S, but no formation of detectable amounts of $CH_4$ was observed under these conditions, as in the case of non-activated photocatalyst (Table 1, entry 14). Furthermore, when the reaction with the pre-activated photocatalyst was carried out at 217.6 °C the production was of 12.45 mmol/$g_{Ru}$, significantly lower than the 64.33 mmol/g measured for the fresh Au-Ru-S material (Table 1, entre 15).
On the other hand, in order to further investigate the role of the Au and Ru NPs in the Au-Ru-S photocatalyst, the $CH_4$ production in the photoassisted methanation reaction using Ru supported on Siralox® (Ru-S) lacking Au NPs was measured. The $CH_4$ production using Ru-S was 30.17 mmol/$g_{Ru}$ about 18 % lower than the productivity value of 36.93 mmol/$g_{Ru}$ obtained at 217.6 °C under the same conditions using Au-Ru-S (Table 1, entries 6 and 7, respectively). This is indicating that Au NPs contributes favorably to the $CH_4$ formation at these reaction conditions, but that the active sites of the methanation are really Ru NPS. Further support to the role of Ru NPs as the active site was obtained by carrying out a control experiment with Au NPs supported on Siralox® (Au-S) in the absence of Ru NPs, whereby it was observed that $CH_4$ formation was practically negligible if compared with production using Au-Ru-S at identical conditions (Table 1, entries 6 and 8). Therefore, it can be assumed that in Au-Ru-S there is a synergic effect between the Au NPs, which shows a very low photocatalytic activity by their own, and the Ru NPs that undergo an enhancement of their photocatalytic activity due to the effect of Au NPs.

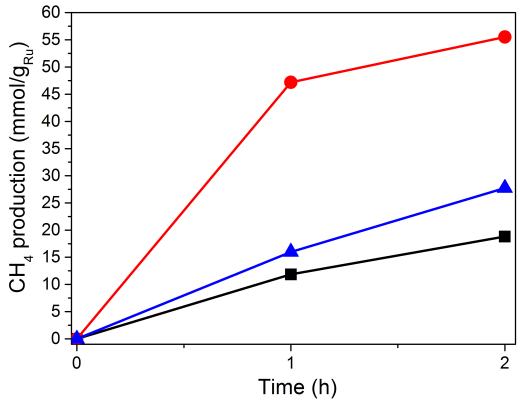


**Figure 7.** $CH_4$ production using Au-Ru-S photocatalyst at 217.6 $^oC$ upon 100 mW/cm$^2$ light intensity (red circles), dark conditions (black squares) and using a 420 nm cut-off filter (blue triangles) (light intensity 94 mW/cm$^2$). $P_{CO2}$=0.25, $P_{H2}$=1.05. Photocatalyst 20 mg (Ru 0.2 wt%, Au 4.1 wt%).

In a similar control experiment, the photocatalytic activity of Ru-S was measured at 217.6 $^oC$, observing that also for this material the formation of $CH_4$ was 32 % lower under the dark than under 100 mW/cm$^2$ irradiation (Table 1, entries 7 and 9, respectively). Therefore, it is reasonable to assume that the light contribution in the photocatalytic activity of Au-Ru-S in the methanation reaction arises from the photoresponse of both Au and Ru NPs, being probably the Au NPs more active in the visible region due to its strong plasmon visible band centered at 529 nm as depicted in Figure S1b in supplementary information. This was further proved by performing a photoassisted methanation experiment at 217.6 $^oC$ using Ru-S and Au-Ru-S using visible light, whereby no enhancement was observed for Ru-S, while the methanation production for Au-Ru-S enhanced by 15 % due to visible light irradiation. These experiments indicate, on the other hand, that a large percentage of the photoresponse observed using the output of the Xe lamp is due to the contribution of the UV region.

To address this issue of visible light activation, an additional irradiation for the $CO_2$ methanation under visible light using a 420 nm cut-off filter (meaning that UV radiations are removed and only visible light illuminates the photocatalyst in this experiment) was performed using Au-Ru-S as photocatalyst at 217.6 $^0C$ under 100 mW/cm$^2$. Under these conditions the $CH_4$ production was approximately reduced to the half, as can be observed in Figure 7. This result indicates that Au-Ru-S shows photocatalytic activity in the visible region of the spectrum.

In order to further study the spectral response of the Au-Ru-S photocatalyst, $CO_2$ methanation was carried out using monochromatic light irradiation of approximately constant intensity of 100 mW×cm$^{-2}$. The results are presented in Figure 8, where the differences in VH4 formation rate have to be attributed to the intrinsic photoresponse of the catalyst and not to differences in the light intensity. As can be observed the photocatalytic activity of Au-Ru-S presents a maximum at 550 nm. Comparison of the photoresponse spectrum shown in Figure 8 with the UV-Vis diffuse reflectance spectrum (Figure 8 inset) revealed that this maximum matches with the Au plasmon band. It is, however, notable that the photoresponse spectrum in the UV region was considerably lower than expected based on the absorption spectrum. This could be due to the overlap of the Siralox® absorption with the Ru and Au NPs absorbance in this region, taking into account that the Ru and Au content is of 0.3 and 4.3 wt%, respectively and, therefore, the absorption in this region is mostly due to inert Siralox. In any case, the UV region does not correspond to plasmon band of Au NPs.

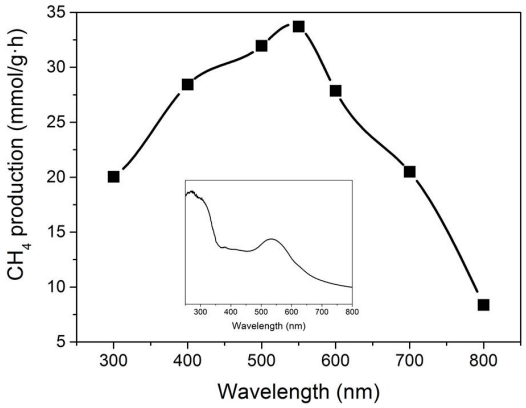


Figure 8. Photoresponse spectrum for to $CH_4$ production of Au-Ru-S after 1 h reaction at 217.6 $^oC$ upon 100 mW/cm$^2$ light irradiation. Reaction conditions: $P_{CO2}$=0.25, $P_{H2}$=1.05. Photocatalyst 20 mg (Ru 0.2 wt%, Au 4.1 wt%).

## Conclusions

It has been demonstrated that the Au-Ru-S material is very active and selective in the $CO_2$ methanation to $CH_4$ at temperatures below 276.6 $^0$C. The $CH_4$ production increases notably upon UV-Vis light irradiation at temperatures of 217.6 $^o$C or higher, although the light contribution to the $CH_4$ production decreases as temperature increases. Experiments at different light intensities provided firm evidence of photoassistence overimpossed with thermal dark reaction. Control experiments using Au-S material exhibited negligible $CH_4$ production, while Ru-S has shown thermal and photocatalytic activity towards $CO_2$ methanation, demonstrating that Ru NPs are the active sites for the $CO_2$ methanation reaction and Au and Ru NPs present a synergic effect. In addition, although the light contribution in the overall $CH_4$ production arises from the photoresponse of both Ru and Au NPs, Au NPs harvest especially in the visible region of the electromagnetic spectrum as consequence of its strong plasmon band. Visible light absorption is particularly important for solar light photocatalysis. Therefore, the visible radiation absorbed by Au would be converted into heat enhancing the overall activity of neighbor Ru NPs.

## Experimental Section

**Materials and procedure.**

Tetrachloroauric acid hydrate (HAuCl4,xH2O) (99.9% purity) was obtained from Acros Aesar. Oleylamine (9-octadecenylamine) (80-90% C18 content, 97% primary amine content) was obtained from Acros and Siralox 5/320 from Sasol Germany. Ru(COD)(COT) was purchased from Nanomeps Toulouse. THF (Sigma-Aldrich) was purified before use by distillation under argon atmosphere.

Au(OA) Synthesis

100 mg (0,30 mmol) of HAuCl•3H20 and 2.8 mL (7.4 mmol) of oleylamine were solved in 2 mL of toluene. The mixture was quickly injected into a boiling solution of 5.8 mL (12.8 mmol) of oleylamine in 98 mL of toluene. The reaction was kept at 110 °C for 2 h. Then, ethanol was added to the resulting deep red solution. Nanoparticles were isolated after centrifugation and were redissolved in 5 mL of toluene afterwards.

Impregnation of Au(OA) in Siralox

The particles were impregnated in 400 mg of Siralox. After 1 night of stirring, the supernatant was removed. The resulting powder was washed 3 times with THF and dried under vacuum.

Decomposition of Ru(COD)(COT) in Au-Siralox

In a glove box, 30mg of Ru(COD)(COT) dissolved in 5 mL of THF were added to 200mg of Au-S. After 1h of stirring, the Fischer-Porter bottle was charged with 3 bar of $H_2$. The color of the powder change from red to black-brown. After a night under $H_2$, the bottle was degassed. The powder was washed 3 times with THF and dried under vacuum.

**Characterization.**

Powder XRD patterns were recorded on a Shimadzu XRD-7000 diffractometer using Cu Kα radiation ((λ = 1.5418 Å, 40 kV, 40 mA) at a scanning speed of 1 $^0$ per min in the 10-80$^0$ 2θ range.
Diffuse reflectance UV-Vis spectra (DRS) in the range of 200 – 800 nm were recorded on a Cary 5000 spectrophotometer from Varian.
The amount of gold and ruthenium present in the Au-ru.s photocatalyst was determined by inductively coupled plasma-optical spectrometry (ICP-OES) by immersing the samples into *aqua regia* for 12 h and analyzing the metal content of the resulting solution.

**Photo-assisted reactions.**

A quartz photoreactor (51 mL) equipped with a nickel alloy thermocouple connected to a heating mantle and temperature controller was loaded with the Au-Ru-S photocatalyst and located under the light spot. $H_2$ and $CO_2$ were introduced in stoichiometric amounts up to achieve a final pressure of 1.3 bar. Prior irradiation the photoreactor was heated at different temperatures, and when the desired temperature was stabilized the photocatalyst was irradiated from the top (6 cm above) through a fiber optics with UV-Vis light from a 300 W Xe lamp. Note that the time required before temperature equilibration can be about 20 min. At that moment the lamp was switched on and this was the initial time of the experiments. No change in the gas phase composition was observed during the period of temperature equilibration in the dark. The $CH_4$ formation was followed by direct measurement of the reactor gases with an Agilent 490 MicroGC having two channels both with TC detectors and Ar as carrier gas. One channel has MolSieve 5A column and analyses $H_2$. The second channel has a Pore Plot Q column and analyses $CO_2$, CO and up to $C_4$ hydrocarbons. Quantification of the percentage of each gas was based on prior calibration of the system injecting mixtures with known percentage of gases.

## Acknowledgements

D. M., J.A. and H.G. thanks financial support by the Spanish Ministry of Economy and Competitiveness (Severo Ochoa SEV2016-0683 and CTQ2015-69563-CO2-1), Generalitat Valenciana (Prometeo 2017-083). JA and D.M. also thank UPV for postdoctoral scholarship and Spanish Ministry of Science for PhD Scholarship, respectively. This project has received funding from the European Research Council (ERC) under the European Union's Horizon 2020 research and innovation programme (grant agreement No GA694159 MONACAT).

**Keywords:** photocatalysis • $CO_2$ methanation • nanoparticles • plasmon band • visible light

[1] D. Lips, J. M. Schuurmans, F. Branco dos Santos, K. J. Hellingwerf, *Energy & Environmental Science* **2018**, *11*, 10-22.
[2] aA. Rose, Z. Huijun, W. Dan, W. Lianzhou, *Advanced Energy Materials* **2017**, *7*, 1703091; bS. A. Han, A. Sohn, S.-W. Kim, *FlatChem* **2017**, *6*, 37-47.
[3] aW. Feifan, L. Qi, X. Dongsheng, *Advanced Energy Materials* **2017**, *7*, 1700529; bB. Wang, W. Chen, Y. Song, G. Li, W. Wei, J. Fang, Y. Sun, *Catalysis Today* **2018**, *311*, 23-39.
[4] K. Takanabe, *ACS Catalysis* **2017**, *7*, 8006-8022.
[5] R. Jingrun, J. Mietek, Q. Shi‐Zhang, *Advanced Materials* **2018**, *30*, 1704649.
[6] aH. Yang, C. Zhang, P. Gao, H. Wang, X. Li, L. Zhong, W. Wei, Y. Sun, *Catalysis Science & Technology* **2017**, *7*, 4580-4598; bK. Sordakis, C. Tang, L. K. Vogt, H. Junge, P. J. Dyson, M. Beller, G. Laurenczy, *Chemical Reviews* **2018**, *118*, 372-433.
[7] M. Götz, J. Lefebvre, F. Mörs, A. McDaniel Koch, F. Graf, S. Bajohr, R. Reimert, T. Kolb, *Renewable Energy* **2016**, *85*, 1371-1390.
[8] K. Ghaib, K. Nitz, F.-Z. Ben-Fares, *ChemBioEng Reviews* **2016**, *3*, 266-275.
[9] aM. Schoder, U. Armbruster, A. Martin, *Chemie Ingenieur Technik* **2013**, *85*, 344-352; bG. A. Mills, F. W. Steffgen, *Catalysis Reviews* **1974**, *8*, 159-210.
[10] aS. Zhang, L. Li, S. Zhao, Z. Sun, J. Luo, *Inorganic Chemistry* **2015**, *54*, 8375-8379; bS. Shunsuke, M. Takeshi, S. Shu, K. Tsutomu, M. Tomoyoshi, *Angewandte Chemie International Edition* **2010**, *49*, 5101-5105.
[11] J. Ren, S. Ouyang, H. Xu, X. Meng, T. Wang, D. Wang, J. Ye, *Advanced Energy Materials* **2017**, *7*, n/a-n/a.
[12] A. Meffre, B. Mehdaoui, V. Connord, J. Carrey, P. F. Fazzini, S. Lachaize, M. Respaud, B. Chaudret, *Nano Letters* **2015**, *15*, 3241-3248.
[13] R. Torres-Mendieta, D. Ventura-Espinosa, S. Sabater, J. Lancis, G. Mínguez-Vega, J. A. Mata, *Scientific Reports* **2016**, *6*, 30478.
[14] B. Alexis, L. Lise‐Marie, F. Pier‐Francesco, C. Julian, S. Katerina, C. Bruno, *Angewandte Chemie International Edition* **2016**, *55*, 15894-15898.
[15] aD. Ugur, A. J. Storm, R. Verberk, J. C. Brouwer, W. G. Sloof, *The Journal of Physical Chemistry C* **2012**, *116*, 26822-26828; bD. Mateo, J. Albero, H. Garcia, *Energy & Environmental Science* **2017**, *10*, 2392-2400.